PROCEEDINGS OF SCIENCE

A Precision Optical Calibration Module for IceCube-Gen2

The IceCube-Gen2 Collaboration[†]

[†] *http://icecube.wisc.edu/collaboration/authors/icrc15_gen2*

E-mail: kai.krings@icecube.wisc.edu

A next generation of IceCube is under design including the Precision IceCube Next Generation Upgrade (PINGU) for the neutrino mass ordering and an extended array for astrophysical neutrino sources. A new level of precision is needed in order to guarantee improved performance with respect to IceCube. An improved calibration system will enable a better understanding of the ice and will therefore significantly reduce systematic effects. We present a new instrument called the Precision Optical Calibration Module (POCAM). By keeping the outer topology identical to that of the IceCube Digital Optical Module (DOM), cost-effective construction and deployment is ensured. The design of the POCAM is based on the principle of an inverted integrating sphere. An appropriately placed LED in combination with a diffusing layer on the inside of the sphere results in a nearly homogeneous light emission from the apertures in the spherical housing. The output of the LED is monitored *in-situ* to high precision, ensuring control over the output from the apertures. The POCAM has been simulated and tested in the framework of Geant4. A prototype POCAM is under construction. We report on the status of the POCAM R&D.

Corresponding authors: K. Krings*[1], K. Abraham[1], K. Holzapfel[1], M. Jurkovič[1], E. Resconi[1], J. Veenkamp[1]

[1] *Physik-Department, Technische Universität München, James-Franck-Str., D-85748 Garching, Germany*

The 34th International Cosmic Ray Conference,
30 July- 6 August, 2015
The Hague, The Netherlands

*Speaker.

PoS(ICRC2015)1133

1. Introduction

For the next generation of IceCube (*IceCube-Gen2*) [1], two different detectors are under study: the Precision IceCube Next Generation Upgrade (PINGU) [2] for the determination of the neutrino mass ordering through a precise measurement of atmospheric neutrino oscillations and a high-energy array [3] instrumenting about 10 km^3 volume of Antarctic ice for high-statistics observations of astrophysical neutrino sources. Both share a common Digital Optical Module (DOM) design, which includes a calibration system similar to IceCube: each DOM is equipped with 12 LEDs, pointing radially outward from the DOM. The calibration system will be used to measure the optical ice properties and the DOMs' timing, sensitivity, positions, and orientations. For IceCube, it has provided the level of precision required for the present detector operation. On the other hand, it lacks an *in-situ* monitoring of the emitted light pulses. LED variation over time as well as LED-by-LED variations limit the precision presently obtained in IceCube. We propose here a self-calibrated, homogeneous, pulsed, and multi-wavelength calibration module: the Precision Optical Calibration Module (POCAM). With the POCAM, measurements of the energy scale and resolution will be performed to the percent precision level, and an even more precise understanding of the optical properties of the Antarctic ice and DOM sensitivity will be provided.

2. POCAM performance goals

The POCAM, shown in Fig. 1, is a calibration device, which will be located on the communication/power cable alongside the DOMs. The POCAM's main goal is a homogeneous and fast illumination of a large part of the instrumented ice volume by providing an isotropic pulsed light source. Fast illumination refers to high-peaked light pulses with short decay times.

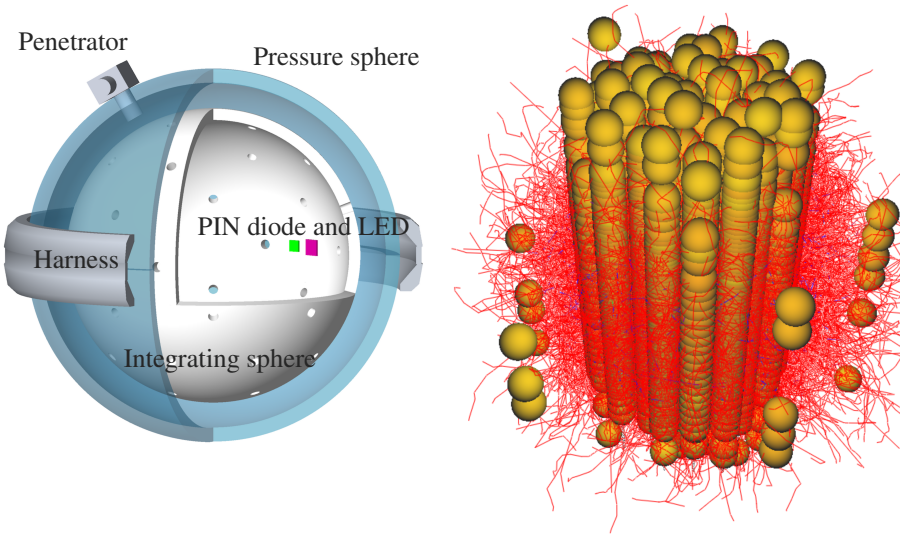

Figure 1: Left: POCAM as a 48 multi-port integrating sphere with a diameter of 24 cm placed in an IceCube pressure sphere. Right: first microsecond of the photon propagation of an idealized isotropic POCAM flash inside PINGU.

Assuming an ideal POCAM, no saturation in the DOMs, and a suitable dynamic range, we want to verify the detector's energy scale and energy resolution[1] at the level of a few percent and measure the absorption and scattering lengths of the Antarctic ice at a level of better than 10 %. The equivalent energy range covered by the POCAM is between a few GeV and some TeV, in the specific case of PINGU. More intense light pulses can be built for a high-energy optimized POCAM. Because the PINGU baseline geometry has a symmetry in the azimuth direction and an up-down asymmetry due to the DOMs' asymmetric construction, we aim for a homogeneous ice illumination on the order of 1 % and 10 % in azimuth and zenith directions, respectively.

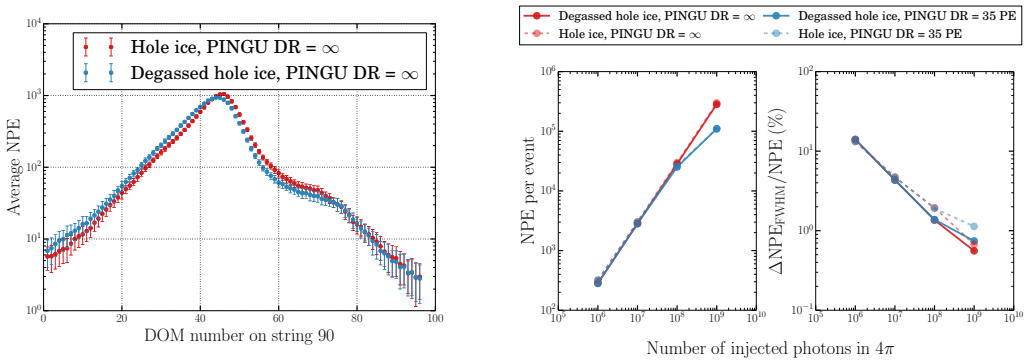

Figure 2: Left: response of DOMs on string 90 to POCAM flashes from the middle of string 88 with 10^9 photons per pulse. Middle: detector response to POCAM flasher pulses of different brightnesses. Right: energy resolution as function of the POCAM brightness. PINGU's dynamic range (DR) was either assumed to be unlimited or restricted to a maximum number of collected photoelectrons (PE) per DOM of 35 PE.

An important design parameter is the light intensity necessary to address the energy scale verification and energy resolution. To answer this question, we have simulated the propagation of individual photons with $\lambda = 405\,\text{nm}$ (IceCube's standard flasher LED) in the Antarctic ice, emitted by an idealized POCAM as an isotropic point-like light source. The photons were propagated from the light source to the individual optical modules of both the existing IceCube and the planned PINGU detectors. For the simulation, we have used the current PINGU baseline geometry [4]. The light source has been placed in the middle of a central PINGU string. We have simulated a light emission with an ideal delta-like time profile yielding between 10^6 and 10^9 photons per pulse. This light intensity is equivalent to a cascade-like physics event with deposited energy between 6 GeV and 6 TeV, respectively. For the light propagation through the Antarctic ice, we have used IceCube's SPICE-Lea [5] ice model in two variations. The first variation labeled as *hole ice* corresponds to the current IceCube refrozen drill hole ice with increased scattering. In the second version, the planned improvement in the drilling technology is taken into account, which should lead to reduced light scattering in newly frozen ice. The latter version is labeled as *degassed hole ice*. The scattering of light in the hole ice affects the amount of light registered by a DOM coming from a particular direction and thus influences the DOMs' angular response. Indeed, this effect is visible in the simulation of light collection for DOMs on string 90, which is the closest neighbouring string to the light source (see Fig. 2, left). The limited dynamic range of the PINGU readout electronics will affect the reconstruction of bright POCAM flashes and thus impact the energy scale verification

[1] Here, energy resolution is defined as $\Delta\text{NPE}_{\text{FWHM}}/\text{NPE}$, where NPE is the number of photoelectrons.

and resolution. To estimate the limiting brightness, we have limited the maximum collected charge to 35 photoelectrons. Such a hard limit is a rather conservative modelling of PINGU's electronics saturation but can be considered as a worst-case scenario. As shown in the middle plot of Fig. 2, in this configuration saturation starts to play a role at flasher brightnesses above 10^8 photons per pulse. In the investigated flasher brightness range, the energy resolution drops from 14 % (10^6 photons per pulse) down to ~1 % (10^8 photons per pulse) (see Fig. 2, right).

3. POCAM components

The POCAM is composed of a light source that has to be intense and fast enough for our purpose here: an *in-situ* light monitoring system that will guarantee a precise knowledge of the light emitted in the ice, a diffusing sphere to generate homogeneous illumination from a discrete light source, and a housing that will allow safe deployment and operation of the POCAM in the deep ice. A matrix of monochromatic fast-switched (few nanoseconds) LEDs with different wavelengths from 370 to 500 nm will be used as a light source. The LEDs are driven by the Kapustinsky circuit [6], which has become popular in astroparticle physics experiments for time and amplitude calibration, including neutrino telescopes (e.g. [7, 8]). This driver is capable of driving LEDs with pulses of few ns FWHM, and the LED provides light pulses with up to 10^9 photons per pulse. This photon yield corresponds to an electromagnetic shower with an energy of ~6 TeV. The light intensity can be controlled only by the applied supply voltage ($V_{CC} < 24$ V). A fast solid state detector such as photodiodes or silicon photomultipliers are implemented in the POCAM in order to continuously *in-situ* monitor the light emitted with a precision of about 1 %. The emitting sphere is composed of an integrating sphere operated in an inverted mode respect the standard one. The highly reflective polytetrafluoroethylene (PTFE) internal layer is used to diffuse the photons from the light source. Multiple ports are then constructed to create a possibly diffused light source. As an alternative to the multi-port setup, a semi-transparent diffusing sphere is also under investigation. To study the performance of the two diffusing sphere options and to optimize the geometry of the POCAM, a dedicated Geant4 [9] simulation has been developed. First results are reported in Sec. 4. The well-tested IceCube pressure sphere is used for the housing of the POCAM. This choice reduces the homogeneity of the POCAM via the presence of the penetrator, the waistband/harness at the equator of the glass sphere, and the cable shadowing, but eases the integration of the POCAM into the standard deployment operations. Presently, a (semi-)transparent waistband and a thinner harness are under study. Moreover, all shadowing influence the measurement at short distances, e.g. at the closest DOMs to the POCAM, but their impact is highly reduced as the distance from the POCAM increases due to photon scattering in ice.

4. POCAM performance study

To optimize the POCAM, a dedicated Geant4 [9] simulation has been implemented. We report here preliminary results of the performance studies done for the multi-port as well as for the semi-transparent layer setup.

4.1 Multi-port setup

As a first step, the POCAM diffusing sphere has been implemented as a multi-port integrating sphere, placed inside the IceCube pressure sphere as shown in Fig. 1. Both volumes are filled with air. The focused light output of the LED, attached to the integrating sphere's inner layer and facing the opposite direction, is diffused inside the integrating sphere after several reflections on the inner diffusing layer and released into the surrounding ice after passing one of the multiple ports in the integrating sphere and the outer pressure sphere. Light homogeneity and timing were investigated by varying the integrating sphere diameter, the number of ports, and the port position and size. The outer pressure sphere has a fixed diameter of 33 cm, and all photons quantities were stored with respect to a reference detection sphere with a diameter of 40 cm. Absorption in both the integrating sphere and the pressure sphere as well as shadowing by the waistband/harness and the penetrator were taken into account. Not studied so far are the influence of the main cable, electronic components inside the POCAM, the hanging assembly, and the port shape. In the simulation, the integrating sphere's thickness has been idealized to be 1 mm. Each port is shaped as a spherical sector with an opening angle α. IceCube's standard 405 nm LED was simulated with a Gaussian wavelength, a uniform cosine-law angular, and a rectangular timing distribution. Wavelength standard deviation, opening angle, and pulse width were adjusted to 10 nm, 10°, and 10 ns, respectively. PTFE with a reflectivity of about 99 %, provided by manufacturers[2], was chosen as the material for the integrating sphere. Values for the pressure sphere's absorption length were taken from IceCube laboratory measurements. The pressure sphere's refractive index of 1.48 was fixed.

Config.	D/cm	n	α/°	T	A	Inhomogeneity		
						$\theta < 60°$	$60° \leq \theta \leq 120°$	$\theta > 120°$
C1	24	768	1	1.46 %	61.0 %	11.9 %	18.5 %	11.6 %
C2	6	768	1	1.46 %	74.4 %	14.7 %	56.4 %	10.3 %
C3	24	768	2	5.85 %	37.3 %	12.9 %	18.9 %	12.1 %
C4	24	192	2	1.46 %	57.7 %	12.3 %	17.8 %	11.6 %
C5	24	–	–	–	50.3 %	12.4 %	14.5 %	12.4 %

Table 1: POCAM configurations: integrating sphere diameter D, number of ports n, port opening angle α, effective photon transparency T, photon absorption A, and inhomogeneity for three different zenith angle zones. Configuration *C5* corresponds to the semi-transparent setup described in section 4.2.

Four different POCAM multi-port configurations listed in Tab. 1 were investigated. The baseline geometry consists of an integrating sphere with a diameter of 24 cm and 768 equidistantly distributed equal ports with an opening angle of 1°, which results in an effective transparency of the integrating sphere to photons of 1.46 %. Effective photon transparency T and photon absorption A are defined as

$$T = n \cdot \frac{\Delta\Omega_{\text{port}}}{4\pi} = n \cdot \frac{1-\cos(\alpha/2)}{2}, \quad A = 1 - \frac{N}{N_0}, \tag{4.1}$$

where n is the number of ports, $\Delta\Omega_{\text{port}}$ the solid angle of one port, α the port opening angle, N the number of photons emitted from the POCAM, and N_0 the number of photons emitted from the LED. In order to avoid too many non-reflected photons, T was restricted to a maximum value of

[2] SphereOptics Zenith Polymer®

about 5 %. The inhomogeneity of the POCAM's photon emission is defined as the ratio of σ and $\bar{N}$, where

$$\sigma = \sqrt{\frac{1}{n_k - 1} \sum_{k \in \Delta\Omega} (N_k - \bar{N})^2}, \quad \bar{N} = \frac{1}{n_k} \sum_{k \in \Delta\Omega} N_k. \tag{4.2}$$

Here, N_k are the emitted photon counts per bin k lying in the solid angle region $\Delta\Omega$ and n_k the number of bins. The inhomogeneity was calculated for the solid angle regions representing the harness shadow and for the regions above and below. Fig. 3 shows the corresponding distributions of the photon emission direction for all POCAM configurations.

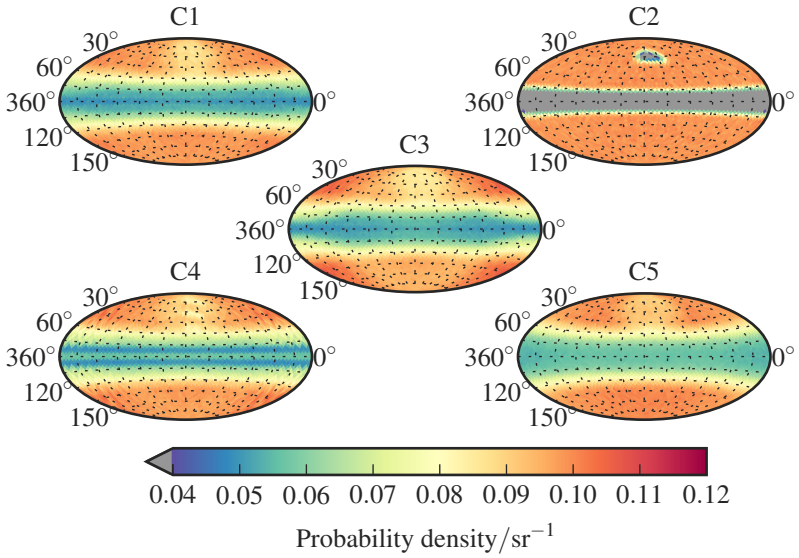

Figure 3: Photon emission direction. In this representation, the LED and penetrator positions are at $\phi = 0°, \theta = 90°$ and $\phi = 180°, \theta = 30°$, respectively. The harness is between $\theta = 79°$ and $\theta = 101°$. Configuration *C5* corresponds to the semi-transparent setup described in section 4.2.

The inhomogeneities due to the shadows of harness and penetrator are clearly visible for zenith angles between 60° to 120° and for azimuth angles below 30° or above 300° in the northern hemisphere, respectively. The shadows get smaller but more pronounced if the size of the integrating sphere is reduced. Except one outlier for configuration *C2* (see Tab. 1), all inhomogeneities are on the order of 10 to 20 %. On average, the baseline configuration gives the best homogeneity. If decreasing the number of ports or increasing the port size, an imprint of the port positions becomes visible as a third source of inhomogeneities due to photons entering the ice without being reflected on the inner diffusing layer or only once. With an integrating sphere diameter of 6 cm for configuration *C2*, almost no photons are emitted horizontally from the POCAM, which explains the large inhomogeneity value of 56.4 %. A different conclusion for the most homogeneous configuration can be drawn, if the shadow regions due to harness and penetrator are not taken into account. Fig. 4 shows the average photon emission direction in azimuth direction for different zenith angle bands. Taking eq. 4.2, configuration *C2* has the smallest deviations in the azimuth direction, which is on the order of 2 %. However, the deviations in the zenith direction are still significantly larger than our requirement of less than 10 %. Thus, the POCAM geometry needs to be further optimized.

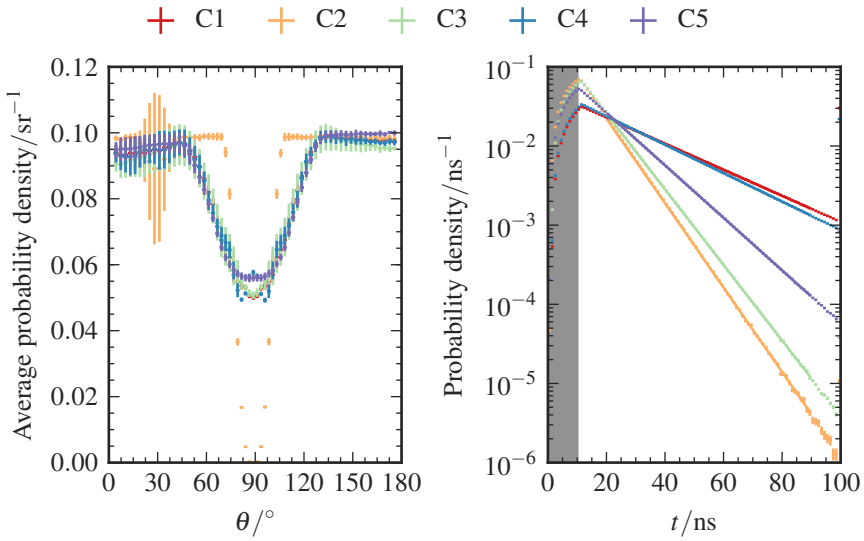

Figure 4: Left: average photon emission direction in azimuth direction for different zenith angle bands. The error bars show the standard deviation. Right: emission time profile. The shaded area refers to the rectangular LED time profile with a width of 10 ns. An exponential distribution is fitted to each time profile for $t > 20$ ns and shown as a solid line.

In Fig. 4, the time profile of configurations *C1* to *C4* are shown. The spectrum is mostly influenced by the effective photon transparency. For a larger ratio of $\Delta\Omega_{\text{port}}/4\pi$, more photons leave the POCAM early. The rising part of the time spectrum is strongly dependent on the emission profile of the LED. The position of the peak is independent of the chosen configuration. Nevertheless, the peak is slightly higher for both configuration *C2* and *C3*. The time distribution falls exponentially after the peak. The decay times are $\tau_1 = 26.4$ ns, $\tau_2 = 8.1$ ns, $\tau_3 = 9.1$ ns, and $\tau_4 = 24.2$ ns. A fraction of the photons leave the integrating sphere earlier, resulting in a higher peak and a shorter decay time τ.

4.2 Semi-transparent setup

The semi-transparency and diffusivity are simulated by defining probabilities for the photon to be either diffusely reflected, diffusively transmitted, or absorbed every time its path coincides with the integrating sphere: P_{refl}, P_{trans}, and $P_{\text{abs}} = 1 - P_{\text{refl}} - P_{\text{trans}}$. To establish diffuse transmission, slight modification to Geant4 have been made. The used probabilities are based on data provided by manufacturers[2]. The probability of diffuse transmission can serve as an analogue to eq. (4.1). As a first result, we present a simulation of a semi-transparent PTFE integrating sphere with $D = 24$ cm, $P_{\text{refl}} = 0.960$, and $P_{\text{trans}} = 0.025$. This simulation produces inhomogeneities listed in Tab. 1 for configuration *C5*. In Fig. 4, the azimuth direction for different zenith angle bands are shown, together with the time profile. The time profile's exponential part has a decay time of $\tau = 13.1$ ns. The time profile of the multi-port baseline configuration is shown for comparison. These simulations show that a semi-transparent PTFE integrating sphere offers advantages over the multi-port configurations. In this configuration, single-reflected photons are as likely as in the port configuration, but independent of the location. The pattern of inhomogeneities is clearly visible for

configuration *C3* and *C4* (see Fig. 3). For configuration *C1* and *C2*, this pattern is present, but less visible. In the semi-transparent PTFE configuration, this pattern is spread out, principally leading to a higher level of homogeneity. This effect is visible in the zenith angle bands (see Fig. 4, left), where the transition from shadow to non-shadow is continuous, whereas it is stepwise for the multi-port configurations. In spite of the clear advantages of a semi-transparent PTFE configuration over the multi-port configurations, conclusive statements would be premature because PTFE is difficult to simulate [10].

5. Conclusions and outlook

We have presented here first ideas and investigations of a new Precision Optical Calibration Module (POCAM). A few POCAM modules deployed uniformly in *IceCube-Gen2* at different depths will help to verify the energy scale and resolution of the future arrays and to determine the optical properties of the South Pole ice with a superior precision compared to present values. With the dedicated POCAM simulation in Geant4, we are able to draw first conclusions on the design of the POCAM geometry: the POCAM configuration consisting of an integrating sphere with a diameter of 6 cm and 768 equidistantly distributed ports with an opening angle of 1° gives the most homogeneous photon emission with inhomogeneities on the order of 2 % in the azimuth direction, which is close to the level of precision we want to achieve; the 6 cm integrating sphere results in a timing with fast rising edges, which are suitable to trigger the continuous pulse monitoring, and decay times below 10 ns; and the POCAM configuration as a semi-transparent diffusing sphere gives also positive results showing a photon emission which is not restricted to discrete locations. The homogeneity in the zenith direction has still to be improved in order to reach a precision of less than 10 %. However, this requirement may be relaxed if photon scattering in the ice is taken into account. Following these first encouraging achievements, we plan to complete the design study and to enter the prototyping phase soon.

References

[1] **IceCube-Gen2** Collaboration, M. Aartsen et al., arXiv:1412.5106.

[2] **IceCube-PINGU** Collaboration, M. Aartsen et al., arXiv:1401.2046.

[3] **IceCube-Gen2** Collaboration, E. Blaufuss et al., *PoS(ICRC2015)1146 these proceedings* (2015).

[4] **IceCube-Gen2** Collaboration, K. Clark et al., *PoS(ICRC2015)1174 these proceedings* (2015).

[5] **IceCube** Collaboration, D. Chirkin, *Evidence of optical anisotropy of the South Pole ice*, in *Proceedings of the 33rd International Cosmic Ray Conference*, 2013. arXiv:1309.7010.

[6] J. Kapustinsky et al., *Nucl. Instrum. Meth.* **A241** (1985), no. 2–3 612–613.

[7] **ANTARES** Collaboration, M. Ageron et al., *Nucl. Instrum. Meth.* **A578** (2007) 498–509, [astro-ph/0703355].

[8] F. Ritter et al., *Nucl. Instrum. Meth.* **A617** (2010), no. 1–3 420–421.

[9] **GEANT4** Collaboration, S. Agostinelli et al., *Nucl. Instrum. Meth.* **A506** (2003) 250–303.

[10] A. K. Soper et al., *Journal of Physics: Condensed Matter* **25** (2013), no. 45 454219.